



Mechanical Behavior of Hybrid Composite Phenolic Foam

Amit Desai, Maria L. Auad, 1 Hongbin Shen and Steven R. Nutt*

Gill Foundation Composites Center, Department of Chemical Engineering and Materials Science, University of Southern California, 3651 Watt Way VHE-602, Los Angeles, CA 90089-0241, USA

* E-mail: nutt@usc.edu

Abstract: Hybrid composite phenolic foams are reinforced with chopped glass and aramid fibers in varied proportions. The mechanical properties are measured and compared with those of foams reinforced with only aramid and glass fibers. The compression and shear properties of the hybrid reinforced foams are also compared with those of commercial polyurethane foams. The reinforced hybrid phenolic foams exhibit greater resistance to cracking and are significantly stiffer and stronger than foams with only glass and Nomex[®] fibers. In general, the mechanical properties of reinforced hybrid phenolic foams are comparable to that of commercial polyurethane foam of equivalent density. The experimentally observed compressive properties (compression modulus) of reinforced phenolic foam with different fiber loading have been compared with existing theories of reinforcement. Composite models such as parallel, series, Halpin–Tsai, and the Hirsch model have been evaluated to fit the experimental data. The findings presented here, coupled with earlier results, demonstrate the potential use of hybrid composite foams as a low-cost engineering material that is tough, strong, and fire retardant.

Key words: foams, glass fibers, aramid fibers, mechanical properties.

1. INTRODUCTION

Hybrid composites in recent times have been developed by using more than one type, shape, or size of reinforcement. These composites have been developed to bestow synergistic properties of Please cite the article as: A. Desai, M.L. Auad, H. Shen, and S.R. Nutt, “**Mechanical Behavior of Hybrid Composite Phenolic Foam,**” J. Cellular Plastics 44 [1] (2008) 15-36. DOI: **10.1177/0021955X07078021**



the chosen fillers and matrix. The study of these hybrid composites is relatively new. The development of composites containing more than one type of fiber reinforcement (hybrid composites) is motivated by the ability to combine advantageous features of various fiber types, including improved performance as well as reduced weight and cost. Understanding the mechanical properties of hybrid composites is essential in order to optimize the design of new hybrid materials [1].

Hybrid composites are gaining commercial significance for several reasons. First, a wider spectrum of tailor-made physical and mechanical properties is possible, thus facilitating the design of materials with specific properties matched to an end use. Second, there are economic advantages replacing a more expensive reinforcement or filler with cheaper materials. Third, hybrids can achieve synergistic effects and improvements in mechanical and functional properties [2].

The properties of hybrid composites depend on several factors, including the interaction of fillers with the polymeric matrix, shape and size (aspect ratio) of fillers, and orientation of fillers, to name a few. For example, hybridizing glass fiber composites with carbon fiber is known to enhance fatigue performance and environmental resistance compared to all glass composites [3]. The judicious selection of banana and sisal fibers has been useful in developing value-added and cost-effective hybrid composites having high tensile and flexural properties [4].

Because of the added complexity of hybrid composites, however, the understanding of mechanical properties, such as strength, modulus, and fracture toughness poses a challenge. As a crude estimate, a rule of hybrid mixtures (ROHM) can be used to predict the properties for a hybrid system consisting of two constituent composites [5].



$$P_H = P_A V_A + P_B V_B \quad (1)$$

where, P_H is the property of the hybrid material, P_A the corresponding property of the first constituent composite, and P_B the corresponding property of second constituent composite. V_A and V_B are the relative hybrid volume fraction of the first and second constituents, respectively, and $V_A + V_B = 1$. A positive or negative hybrid effect is described as a positive or negative deviation of a certain mechanical property from the ROHM [5].

Phenolic foam has been considered in the current research. Phenolic foam has certain distinct advantages when compared with other polymeric foams. For example, phenolics exhibit excellent fire resistance, including low flammability, low peak heat release rate (PHRR), no dripping during combustion, low smoke density, and low toxicity [6]. In addition, phenolic foam is one of the less expensive polymer foams commercially available. Phenolic foam is also thermally stable over a broad temperature range, maintaining performance and stability from -196 up to 200 °C. The thermal conductivity is low, which has led to a broad range of applications as an insulating material. Finally, phenolic foam is highly resistant to chemicals and solvents [6]. However, structural applications of phenolic foam have been severely limited because of the inherent brittleness and friability [7]. As a consequence, phenolic foam is rarely used as a core material in sandwich structures.

In contrast, polyurethane (PU) foam is widely used for sandwich cores in structural applications. PU foam can be moderately stiff and easy to process. However, PU foam is highly flammable and produces toxic fumes during combustion, a factor that precludes many practical uses. In contrast, phenolic foam exhibits excellent fire resistance, including low flammability, but poor toughness and friability characteristics. At present, there is a need for fire-retardant, non-toxic



foam for use in fire-critical sandwich structure applications. Furthermore, standards for fire, smoke, and toxicity (FST) properties are becoming increasingly stringent worldwide, and limitations of conventional structural foams may preclude their continued use.

Over the past few decades, there have been attempts to increase the toughness of phenolic foams [6,8]. Particularly, short fiber reinforcement of phenolic foam was considered [9,10]. Significant improvements in peel strength and toughness were achieved by reinforcing phenolic foam with aramid fibers [7] (e.g., Nomex[®] and/or Kevlar[®]), which have well-known affinity for phenolic foams. For example, Shen et al. found that the addition of only 3 wt% short aramid fibers produced a six-fold increase in peel strength, and addition of 5 wt% fibers resulted in a seven-fold increase over unreinforced foams. Furthermore, increasing the fiber length and the fiber loading generally increased the toughness. Interestingly, aramid fibers were more effective than glass fibers in enhancing the peel strength and abrasion resistance for equivalent loadings and fiber length, while glass fiber additions enhanced foam strength, stiffness, and dimensional stability [9,10]. Based on the above observations, it is hypothesized that the mixed use of glass and aramid fibers in hybrid phenolic foams could produce an optimal combination of toughness and strength.

In this study, property enhancements observed in hybrid phenolic foams reinforced with glass and aramid fibers blended in varied proportions are reported. The properties of the hybrid composite foams are assessed to determine the effects of blending different fibers in different proportions. Properties are compared with foams having only aramid or glass fibers. In addition, reinforced phenolic foams are compared with polyurethane foams in order to assess the potential of the material as a fire-retardant, non-toxic substitute in fire-critical structural applications. The present work also includes attempts to fit the mechanical properties of hybrid foam into some existing models of composite materials [11].

Please cite the article as: A. Desai, M.L. Auad, H. Shen, and S.R. Nutt, “**Mechanical Behavior of Hybrid Composite Phenolic Foam,**” *J. Cellular Plastics* 44 [1] (2008) 15-36. DOI: **10.1177/0021955X07078021**



2. EXPERIMENTAL DETAILS

2.1. Foam Preparation

Phenolic foams were synthesized using a proprietary formulation [12] and a patented technology [13]. The formulation was typically composed of phenolic resole resin (solid content >80%) and appropriate amounts of pentane to achieve desired foam densities. Polysulfonic acid (PSA) was used as a catalyst for the reaction. When fiber reinforcements were introduced, the amount of PSA catalyst was slightly increased to allow more time for dispersing fibers. All foams were formulated to achieve a density between 190 and 250 kg/m³ (12–15 pcf).

The synthesis of reinforced phenolic foam sample was carried out by blending chopped fibers with the phenolic resin using a high-speed dual axis mixer, as described previously [13]. The glass fibers (Lauscha Fiber International) were 6.4 mm in length and 11 mm in diameter, and were treated with a silane coupling agent. Aramid fibers (DuPont Nomex[®]) were 6.4 mm in length and ≈12 μm in diameter. After blending fibers and resin with around 2 min of mixing time, the mixture was then poured into a mold and held at 80 °C for 1 h. The foams were further neutralized overnight in a closed chamber with a source for ammonia.

2.2. Mechanical Tests

Test specimens were sectioned from foam slabs using a diamond blade band saw. Special attention was given to the cutting direction with respect to the foam rise direction, and the edges of foam blocks were avoided. Mechanical tests were performed using a universal testing machine (Instron 1331) in accordance with ASTM standards.

Compression testing was performed in accordance with ASTM D1021. Compressive modulus was taken as the steepest initial slope of the stress–strain curve, and strength was determined from



the maximum load (in a range of strain <10%). At least five replicates were tested for each specimen, and the results were presented as the average value of all replicates.

Lap shear testing was performed in accordance with ASTM C273 [14]. Foam specimens were bonded to stainless steel plates with a fast-cure epoxy adhesive. The shear modulus was taken as the steepest slope of the stress–strain curve, and strength as the peak stress value. At least five replicates were tested for each specimen, and the results were presented as the average value of all replicates.

2.3. Morphology

Foam surfaces were examined by scanning electron microscopy (SEM, Cambridge 360). Prior to sectioning, samples were submerged in liquid nitrogen to avoid structural deformation and damage to the foam microstructure. Subsequently, samples were sputter-coated with gold to impart electrical conductivity and reduce charging artifacts. The operating voltage of the SEM was 10 kV.

3. RESULTS AND DISCUSSION

3.1. Compression Tests

Like most plastic foams, phenolic foam exhibits a multi-stage deformation response when subjected to compressive loading [15]. An initial steep rise in the stress–strain curve is followed by a constant-stress plateau, during which cells collapse by the bending and buckling of cell walls and edges. The effect of fiber type, fiber proportion, and (loading direction) anisotropy are described in the following subsections.

3.2. Fiber Type Effect

The fiber type had a distinct effect on the compression behavior of the hybrid composite foams, as shown in Table 1. For compression properties measured parallel to the foam-rise



direction, glass fibers produced greater enhancements in compressive properties than aramid fibers. For example, glass fiber-reinforced foams showed strength increase of almost 275% (compared with unreinforced foams), while the increase in strength was 36% for aramid fiber foams. Glass fiber reinforcement also resulted in a 130% increase in compression modulus, while aramid fiber reinforcement produced no significant change. This phenomenon can be attributed in part to the relatively high stiffness of glass fibers [17] compared with aramid fibers [16], and to a higher degree of glass fiber orientation along the foaming direction. Evidence of preferred orientation of glass fibers was reported by Shen et al. [18], using micro computerized tomography (CT) imaging of composite foam.

Table 1. Compressive properties of foams (density = 190–240 kg/m³).

Foam Formulations (% weight)	Parallel ^a		Perpendicular ^a		Modulus anisotropy ratio E /E _⊥
	Modulus (MPa)	Strength (MPa)	Modulus (MPa)	Strength (MPa)	
Phenolic Unreinforced (14 pcf)	37.20±4	0.92±0.05	18.26±2	0.62±0.04	2.03
5% Nomex® reinforced (12.5 pcf)	35.04±3	1.25±0. L5	32.40±2	0.91±0.08	1.08
1.25% glass + 3.75% Nomex® (13 pcf)	60.05±5	3.05±0.35	51.06±4	2.65±0.30	1.17
2.5% glass + 2.5% Nomex® (13.5 pcf)	79.17±5	3.26±0.40	54.65±5	2.75±0.35	1.45
3.75% glass + 1.25% Nomex® (13.5 pcf)	84.15±7	3.40±0.30	52.26±3	3.11±0.45	1.61
5% Glass reinforced (13 pcf)	85.20±3	3.45±0.20	28.85±2	3.18±0.15	2.95
Polyurethane ^b (14 pcf)	101	3.11	65.2	2.51	1.54

a Loading direction with respect to foam’s original foaming direction.

bData from manufacturer’s datasheets [21].

3.3. Anisotropy

The anisotropy of foam properties is apparent from the data in Table 1. For example, in the direction normal to the foam rise direction, the glass fiber foam showed an increase in modulus of 156% (vs. a 275% increase for the foam rise direction), and virtually the same strength in the two Please cite the article as: A. Desai, M.L. Auad, H. Shen, and S.R. Nutt, “Mechanical Behavior of Hybrid Composite Phenolic Foam,” J. Cellular Plastics 44 [1] (2008) 15-36. DOI: [10.1177/0021955X07078021](https://doi.org/10.1177/0021955X07078021)



directions. However, for the aramid fiber foam, the modulus in the foam rise direction was identical to the unreinforced foam, while in the normal direction, the composite foam showed a 77% increase. The strength increase was 36 and 47% for the foam rise and normal directions. From these observations, it appears that the aramid fibers may not align in the foam rise direction to the same extent that the glass fibers do, although this assertion is speculative at present.

Gibson and Ashby [15] noted that most foams, especially those produced by an open mold process, are anisotropic in the foaming and transverse directions. The anisotropy may arise from two independent factors: foam structure and materials. Using an elongated cubic foam cell mode, they derived a Young's modulus anisotropy ratio that depended on the structural anisotropy alone, as shown in Equation (2).

$$\frac{E_{\parallel}}{E_{\perp}} = \frac{2R^2}{[1 + (1/R)^3]} \quad (2)$$

where E_{\parallel} is the Young's modulus of the foam measured parallel to the foaming direction, E_{\perp} is the Young's modulus perpendicular to the foaming direction, and R is the shape anisotropy ratio, defined as the ratio of cell height (measured in the foaming direction) to cell width (measured in the transverse direction). This relationship is obtained for open-cell foams when the cell membranes are weak relative to the cell edges, and thus their contribution to foam modulus can be neglected [15].

Using the framework described above, the modulus anisotropy ratios of the foams were calculated (Table 1). As the values show, the aramid fiber foams are nearly isotropic, with E_{\parallel}/E_{\perp} approaching 1, whereas the glass fiber foams are substantially anisotropic. For hybrid foams, the modulus anisotropy ratio is ≈ 1 (or slightly higher). The framework can be tested by analyzing PU



foams, which show a shape anisotropy ratio of ≈ 1.2 [15]. Insertion of this R value in Equation (1) yields a modulus ratio, E_{II}/E_{\perp} of 1.62, which compares with the measured modulus ratio of 1.54, as shown in Table 1. This indicates that PU foam behaves like open-cell foam.

If Relationship (2) is valid for plain phenolic foam, the shape anisotropy ratio R should be ≈ 1.25 . However, for the fiber reinforced foams, the property anisotropy should stem from material anisotropy as well as from a structural origin. The presence of fibers may modify the process of cell formation during foaming, altering the foam cell morphology from that of plain foam. Meanwhile, fibers in the foam may acquire preferred orientations and non-uniform distributions, contributing to property anisotropy. This can be observed for the hybrid foam data in Table 1, where preferred fiber orientation of glass and aramid fibers in the foam leads to anisotropy in the foam properties, and the modulus anisotropy ratio varies with change in fiber proportion.

The variation in foam properties for axial and transverse loading directions reflects the extent of fiber alignment, which depends on fiber type. Consequently, the strength and modulus of the glass fiber phenolic foams are greater than those of the aramid fiber counterpart. This result is also consistent for hybrid foams, where an increase in modulus is observed in the parallel direction with increasing proportion of glass fibers. However, when load is applied transverse to the foam rise direction, the hybrid foams have higher modulus than the foams reinforced with either glass or Nomex[®] fibers.

3.4. Proportions

Blending glass and aramid fibers in varied proportions produced hybrid composite foams with significant improvements in modulus and strength over unreinforced foams, as shown in Table 1. The greatest improvements in modulus and strength were observed when glass and aramid fibers were added in the ratio of 3:1, respectively. This ratio resulted in a 126% increase in modulus and

Please cite the article as: A. Desai, M.L. Auad, H. Shen, and S.R. Nutt, “**Mechanical Behavior of Hybrid Composite Phenolic Foam,**” J. Cellular Plastics 44 [1] (2008) 15-36. DOI: **10.1177/0021955X07078021**



a three-fold increase in strength for the hybrid foam (glass: aramid, 3:1) relative to the unreinforced foam (for both axial and transverse directions). Fiber weight ratios of 1:1 and 1:3 (glass : aramid) yielded a nearly two-fold increase in modulus for both types of hybrid foams, and increases in strength of 250 and 230%, respectively. The results indicate significant increases in strength and modulus for the hybrid foam relative not only to unreinforced foams, but also to composite foams reinforced with only aramid fibers.

3.5. Compression Stress–Strain Relationships

Gibson and Ashby [15] have described and analyzed the deformation behavior of cellular materials under compressive loading. Phenolic foam exhibits multistage deformation response when subjected to compressive loading. In Figures 1 and 2, initial part of the compression stress strain response is displayed (strain < 0.2). This is the portion of the deformation response that is most relevant for engineering applications, and contains the key parameters of compressive modulus and strength. The data from several compression tests for hybrid foams have been summarized in Table 1.

3.6. Phenolic versus Polyurethane (PU)

The data from Table 1 afford an opportunity for comparisons with PU foams. Typically, PU foams are stiffer (higher modulus) than most phenolic foams of equivalent density. The compressive modulus of hybrid phenolic foam (glass and Nomex[®] in a ratio of 3:1) in the foam rise direction is only 20% less than PU foam of the same density, while the compressive strength is comparable. Thus, the hybrid composite phenolic foam appears to offer mechanical performance nearly comparable to PU foams, and superior FST properties. Such foams would be useful for sandwich structure applications with stringent FST requirements.

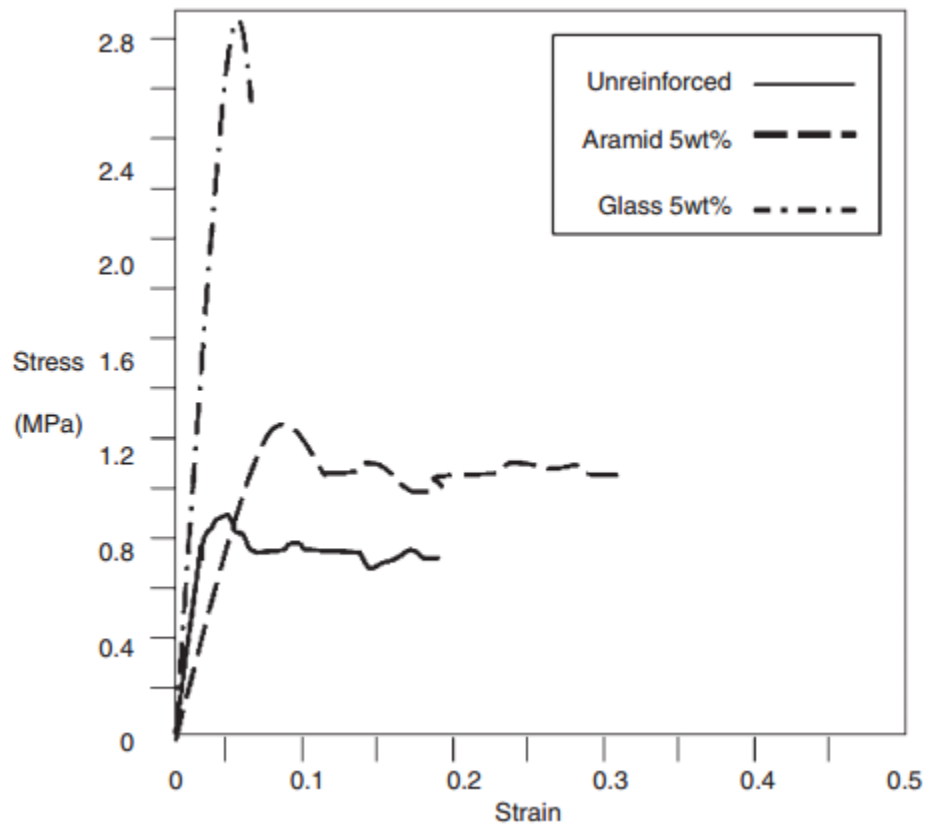


Figure 1. Typical compression stress–strain relationships of phenolic foams. Loading direction is parallel to the foam rise direction.

3.7. Shear Tests

By design, sandwich cores are intended to mechanically couple face sheets by carrying shear loads [19]. Consequently, shear properties are among the most important criteria governing the selection of core materials for sandwich structures. To assess the potential of hybrid composite foams in such structural applications, the shear properties were measured, and these are summarized in Table 2.

3.8. Fiber Type Effects

The hybrid reinforced foams exhibit marked increases in shear modulus and shear strength, as shown in Table 2. The data show that glass fiber reinforcement produces a greater increase in shear



modulus than the aramid fiber counterpart at the same fiber loading. For example, glass fiber composite foam shows a 78% increase in shear modulus and 158% increase in shear strength relative to unreinforced foam. In contrast, the aramid fiber foam shows only a 12% increase in modulus and a 14% increase in strength relative to the unreinforced foam. The shear data were measured only in the plane normal to the foam rise direction, and are consistent with previous reports. For example, Shen et al. [20] found that the shear resistance of fiber-reinforced phenolic foam was substantially greater on the plane normal to the foam rise direction. However, the difference in anisotropy between unreinforced and reinforced foam was small, indicating shear properties of phenolic foam were insensitive to material anisotropy.

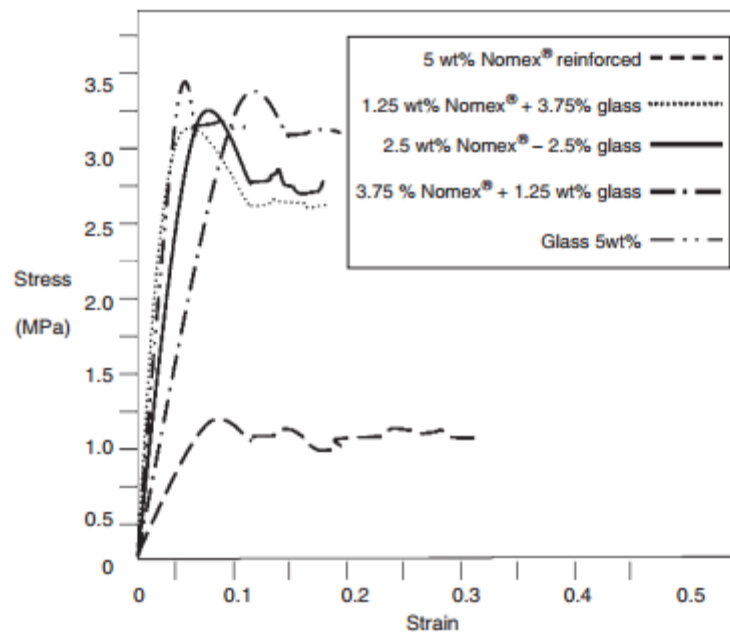


Figure 2. Typical compression stress–strain relationships of phenolic foams. Loading direction is parallel to the foam rise direction.



Table 2. Shear properties of foams (density = 190–240 kg/m³).

Foam formulations	Perpendicular ^a		Strain energy density (J 106 /m ³)
	Modulus (MPa)	Strength (MPa)	
Phenolic Unreinforced (14 pcf)	18.±1.50	0.48±0.04	9.05± 2
5% Nomex [®] reinforced (12.5 pcf)	20.4±3.00	0.55±0.04	22.95±2
1.25% glass + 3.75% Nomex [®] (13 pcf)	30.26±3.0	1.40±0.35	21.78±2
2.5% glass + 2.5% Nomex [®] (13.5 pcf)	54.65±4.5	2.32±0.45	15.3±2
3.75% glass (13.5 pcf) + 1.25% Nomex [®]	35.55±3.5	1.48±0.25	4.45±1
5% Glass reinforced (13 pcf)	32.26±3.5	1.24±0.30	4.03±1
Polyurethane ^b (14 pcf)	30.5	2.1	14.5±2

^aLoading direction with respect to foam's original foaming direction.

^bData from manufacturers datasheets [21].

3.9. Proportions

The shear properties were measured for hybrid foam samples consisting of aramid and glass fibers in weight ratios of 3:1, 1:1, and 1:3. In all three hybrid foams, the shear strength and modulus increased substantially, as shown in Table 2. Hybrid foams with equal proportions of glass and aramid fibers exhibited shear properties superior to the other hybrid foam samples, which included a nearly three-fold increase in shear modulus and a nearly five-fold increase in shear strength. Hybrid foam samples reinforced with glass and aramid fibers in ratios of 1:3 and 3:1 showed increases in shear modulus of 67 and 96%, respectively, and an almost three-fold increase in shear strength.

For hybrid systems in general, both glass and Nomex fibers enhanced the shear properties of the foams. The 1:1 aramid and glass ratio hybrid foams exhibited the highest shear modulus of all the foams tested. From the experimental observations, it is concluded that at the homologous fiber ratio, the hybrid foam system exhibited superior shear modulus compared to other reinforced phenolic foams with varied fiber proportions. Thus, the contribution of both fiber types is critical to the shear performance of phenolic foams. However, when the optimum fiber ratio of 1:1 was



altered, the shear properties decreased by more than 50% compared to glass and Nomex[®] reinforced foams.

For hybrid systems in general, both glass and Nomex[®] fibers enhanced the shear properties of the foams. The 1:1 aramid and glass ratio hybrid foams exhibited the highest shear modulus of all the foams tested. From the experimental observations, it is concluded that at the homologous fiber ratio, the hybrid foam system exhibited superior shear modulus compared to other reinforced phenolic foams with varied fiber proportions. Thus, the contribution of both fiber types is critical to the shear performance of phenolic foams. However, when the optimum fiber ratio of 1:1 was altered, the shear properties decreased by more than 50% compared to glass and Nomex[®] reinforced foams.

3.10. Shear Stress–Strain Relationship

Figure 3 shows typical shear stress–shear strain curves for aramid fiber and glass fiber phenolic foams. The unreinforced foam shows purely elastic behavior, and the glass fiber foam shows similar behavior followed by a brittle failure, although with higher strength and modulus. In contrast, the aramid fiber foam shows a distinctly different failure behavior characterized by more graceful failure. The foam continues to carry load well beyond the peak stress, showing a smooth decline in stress that continues to large shear strains. This behavior is consistent with the report by Shen et al. [20], and indicates substantially enhanced shear toughness. The extensive energy absorption is attributed to the tenacity of the aramid fibers embedded in the foam structure, which bridge the shear cracks and gradually pull out of the foam matrix. The aramid fibers afford greater flexibility and chemical compatibility than the glass fibers, thus accounting for the different behavior of the two composite foams.

As shown in Figure 4, the hybrid composite foams exhibit similar stress–strain behavior. This includes a smooth decline in stress after the peak stress, extending to strains of 15–40%. As the



weight proportion of aramid fiber is increased, the shear modulus decreases, and the peak stress increases. After peak stress, the stress decline becomes smoother and more gradual and the ultimate strain increases significantly. The 3:1 hybrid foam (aramid-to-glass ratio) exhibits the highest peak stress and the largest ultimate strain of the three hybrid foams. The increase in ultimate strain and energy absorption is attributed to the tenacity of the flexible aramid fibers, which resist pullout and result in extensive crack bridging and more graceful failure, manifest as a gradual decline in stress with increasing strain.

Viewed from the opposite perspective, as the glass fiber content in hybrid foams is increased, the ultimate strain decreases. There also is an increasing tendency towards brittle rupture, and a slight but measurable in peak stress. In the limit, i.e., in foams with all glass fibers, brittle rupture is observed, much like unreinforced phenolic foam (Figure 3). However, the shear modulus also increases with increasing glass content.

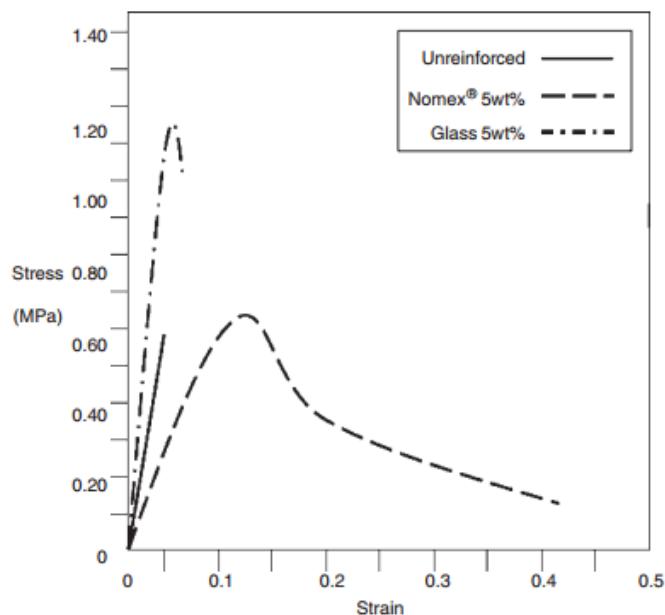


Figure 3. Typical shear stress–strain relationships of phenolic foams. Shear plane and loading direction are both parallel to the foam rise direction.



Energy absorption is an important performance metric for cellular materials, including metal and polymeric foams [15]. The energy absorbed during fracture provides a useful means for comparing foam performance, especially with regard to impact resistance and damage tolerance [22]. Values of strain energy density for the composite foams were calculated from the areas under the stress–strain curves [23], and are listed in Table 2. The strain energy density of aramid fiber foam is 150% greater than that of unreinforced foam. In contrast, the glass fiber foams show a 55% decrease in strain energy density, indicating diminished toughness. Significantly, as aramid fibers are blended with glass fibers, the strain energy density values for the resulting hybrid foams increase with increasing aramid fiber content, nullifying the embrittling effect of the glass fibers. Hybrid foams with 3:1 aramid and glass fiber exhibit a strain energy density nearly 2.4 x greater than plain phenolic foam. The gradual and continuous decline in stress beyond peak stress may translate into improved damage tolerance and more graceful failure of the hybrid foams, both of which are desirable for structural applications.

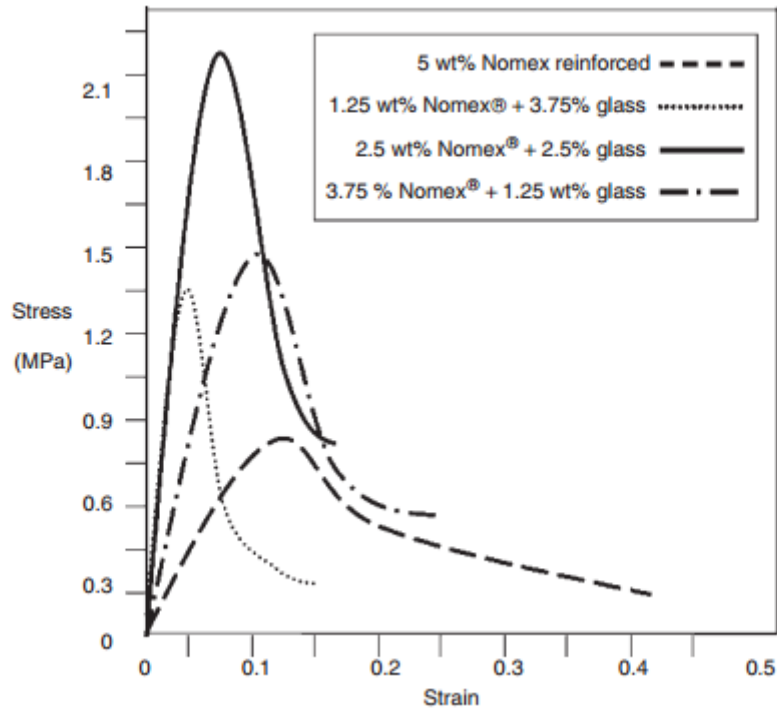


Figure 4. Typical shear stress–strain relationships of phenolic foams. Shear plane and loading direction are both parallel to the foam rise direction.

3.11. Phenolic versus Polyurethane (PU)

Polyurethane foam is a widely used structural foam that is convenient to manufacture and nearly isotropic in shear performance [24]. In the present study, PU foam is selected as an additional benchmark for comparison with the hybrid phenolic foams. The shear modulus of the 1:1 hybrid foam was nearly twice the modulus of the benchmark PU foam of equivalent density. A 10% increase in shear strength was also observed for the 1:1 hybrid foam. The surprising properties of the foams are linked in part to the foam structure, described in Section 3.4.

3.12. Theoretical Modeling of Foam Properties

Several models have been proposed to describe the mechanical properties (compression, tension, etc.) of reinforced composite materials in terms of different parameters [25, 26]. These models can be classified into two groups, one based on the nature of the matrix, and the other



based on the type of reinforcements. According to the parallel and series models, Young's modulus is calculated according to the following equations [31].

Parallel model

$$M_c = M_f V_f + M_m V_m. \quad (3)$$

Series Model

$$M_c = \frac{M_m M_f}{(M_m V_f + M_f V_m)} \quad (4)$$

where, M_c , M_m , and M_f are the Young's moduli of composite, matrix, and fiber, respectively, and V_f and V_m are the volume fractions of fibers and matrix, respectively. The third model considered is the Hirsch model, which is a combination of the parallel and series models [30]. According to this model, the Young's modulus is given by the following equation:

$$M_c = \frac{x(M_m V_m + M_f V_f) + (1-x)M_f M_m}{(M_m V_f + M_f V_m)} \quad (5)$$

where, M refers to the modulus, V is the volume fraction, x is the stress transfer ratio [31], and the subscripts c , f , and m signify the composite, fiber, and matrix, respectively. The Halpin–Tsai model has been used by several researchers to analyze polymeric blends consisting of continuous and discontinuous phases [27]. This model was also useful in determining the properties of composites that contained discontinuous fibers oriented in the loading direction [28,29]. According to the Halpin–Tsai model [28], the stiffness estimate in the fiber direction, E_{II} , is given by

$$\frac{E_{II}}{E_m} = \frac{(1 + \xi \eta v_f)}{(1 - \eta v_f)} \quad (6)$$



where,

$$\eta = \left(\frac{E_f}{E_m - 1} \right) \left(\frac{E_f}{E_m + \xi} \right)^{-1}, \quad \xi = 2 \left(\frac{l}{d} \right)$$

v_f is the volume fraction of fibers, and subscripts f and m refer to fiber and matrix, respectively.

The experimental results obtained from compression tests were plotted with the results obtained by fitting values for the models discussed here. Figure 5 shows the volume fraction of fibers plotted as a function of the compression modulus (parallel direction). Parallel, series, and Hirsch models do not provide good fits to the data, and fail to explain the behavior of hybrid foams. The assumption of uniform stress or uniform strain is clearly an oversimplification in these models, because the stress transfer mechanism in continuous fiber reinforced composites is different from that of short fiber composites [31, 32]. Shen et al. [18] reported that severe breakage of glass fibers occurred during processing of reinforced foams, resulting in a wide distribution of lengths. The Halpin–Tsai model was thus plotted for original fiber length of 6 mm and another arbitrary length of 3 mm. The Halpin–Tsai model for fiber length 3 mm comes close to fitting the experimentally observed behavior of hybrid foams. However, the model lacks the complexity needed to capture the actual behavior, and thus does not accurately predict the dependency of the compression modulus on the volume fraction of fibers. This deficiency can be partly attributed to the complex foam structure, described in the following section.

To reasonably depict the mechanical behaviors of hybrid foams, more advanced modeling techniques are required. The scaling law, for example, has proven useful for modeling complex engineering systems where traditional methods are typically tedious and timeconsuming [33]. The scaling law (SLAW) differs from classical dimensional analysis in that it selects the scaling law with the smallest predictive error out of all the dimensionally correct models. The algorithm

Please cite the article as: A. Desai, M.L. Auad, H. Shen, and S.R. Nutt, “**Mechanical Behavior of Hybrid Composite Phenolic Foam,**” J. Cellular Plastics 44 [1] (2008) 15-36. DOI: **10.1177/0021955X07078021**



combines a linear regression model of the experimental data with physical consideration of the process, namely, that the units of the resulting models match the units of the dependent variable. The output of the algorithm is a physically meaningful and simple power law representing the process, and a set of dimensionless groups ordered by relevance to the problem. Thus, application of SLAW may offer advantages for the study of hybrid foams, as it affords one an opportunity to consider aspects such as fiber length, fiber proportion, and other parameters which directly influence the mechanical performance of foam considered in the same model. Present efforts are aimed at implementing the approach of scaling laws [33] to hybrid foams for achieving a suitable model for the complex behavior of hybrid composite foams.

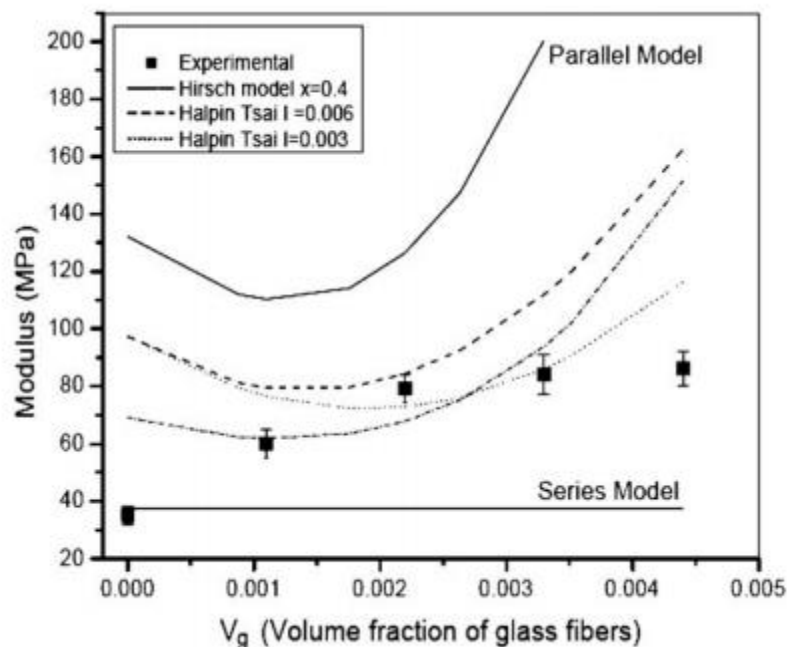


Figure 5. Comparison of experimental results with various theoretical models.

3.13. Foam Structure

Microscopic observations of hybrid foams revealed interactions between the different fiber types, as well as fiber–matrix interactions. Typical observations of fracture surfaces from the 1:1



hybrid foam are shown in Figures 6 and 7. Figure 6 shows details of the interaction between glass fibers and the foam matrix. Fibers appear to be intercellular (between cells), as opposed intracellular (spanning cells), a probable consequence of fiber surface tension during foam expansion. The glass fiber ends protrude from the foam matrix, which shows evidence of damage and cracking in the vicinity. The fibers are largely bare of foam fragments, indicating fiber pullout and failure at the interface. Cracks apparently initiate in the brittle foam and deflect along fiber interfaces before propagating further.

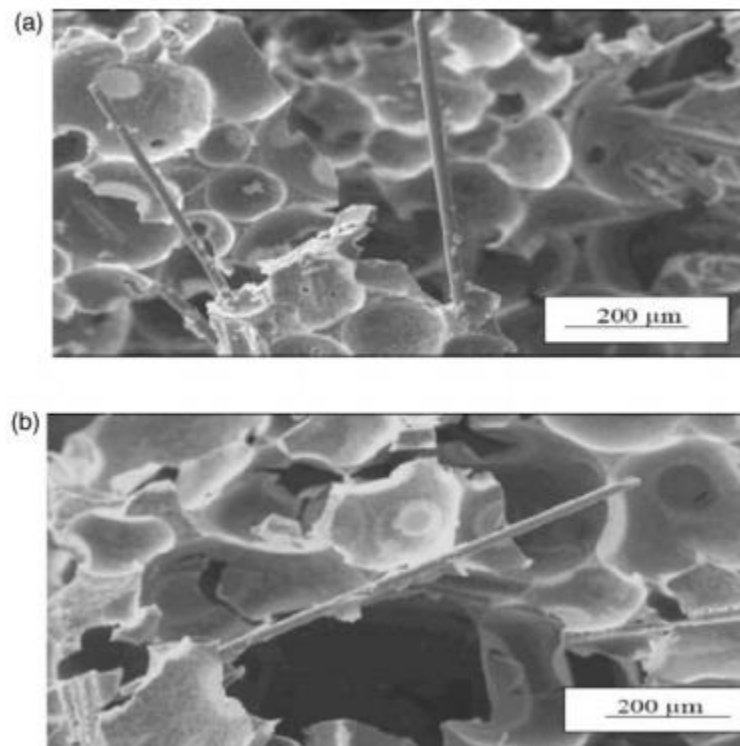


Figure 6. Scanning electron micrographs of glass fibers in the matrix of 'hybrid' foams.

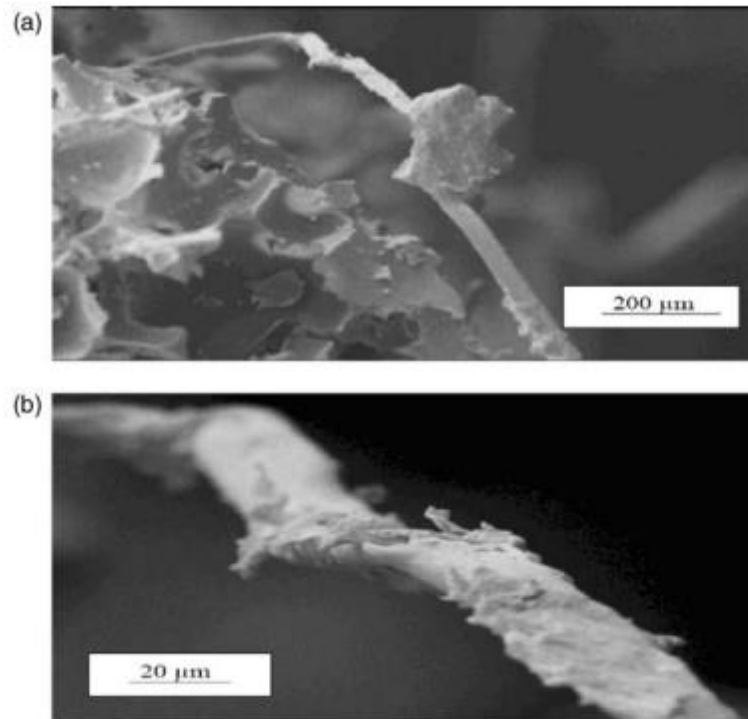


Figure 7. Scanning electron micrographs of Nomex fibers in the matrix of 'hybrid' foams.

A distinctively different phenomenon was observed for aramid fibers in the hybrid foam, as shown in Figure 7. The micrograph shows a foam fragment adhering to an aramid fiber extending from the fracture surface. Adhering to the aramid fiber are numerous small fragments of phenolic foam, indicating unusually strong cohesive strength that forces a combination of interface and matrix failure. Shen et al. [7] reported a micro-peeling process for aramid fiber reinforced foam where tiny fibrils had peeled off from an aramid fiber stem. This phenomenon undoubtedly contributed to the observed property enhancements of hybrid foams. As the micropeeling process proceeds in the hybrid foam, the stress concentration is reduced, and secondary cracks are induced that branch into adjoining regions, thereby enlarging the fragmented or damaged volume. This crack branching, combined with the flexibility of aramid fibers, results in extensive crack bridging in hybrid foams. As a result, failure is more graceful, as evidenced by the stress–strain behavior shown previously in Figure 4. Thus, despite the presence of glass fibers in hybrid foams, the brittle

Please cite the article as: A. Desai, M.L. Auad, H. Shen, and S.R. Nutt, “**Mechanical Behavior of Hybrid Composite Phenolic Foam,**” *J. Cellular Plastics* 44 [1] (2008) 15-36. DOI: **10.1177/0021955X07078021**



quality of failure is significantly diminished, and the foam strength is 1.9 x greater than the plain glass reinforced counterpart at the same density.

4. CONCLUSIONS

Hybrid fiber reinforcement of phenolic foams improves all aspects of shear and compression properties. The optimal fiber ratio for the reinforced hybrid phenolic foam system was the 1 : 1 ratio of glass to aramid fibers. This homologous ratio produces a balance in the shear and compressive properties. The hybrid foam retains toughness and stiffness, with significant enhancement of strength. These properties can be tailored to specific requirements for particular applications simply by varying the fiber proportions. Consequently, the hybrid fiber approach is well-suited to optimizing a broad range of foam properties.

A major issue motivating hybrid fiber reinforcement of phenolic foams concerns the potential suitability of the foams for structural applications. The evaluation of the hybrid composite phenolic foams has shown that the mechanical performance is comparable to commercial PU foams of equivalent density. These results indicate that judicious selection of fiber reinforcements in optimal proportions can yield structural foams that are strong, tough, fire-retardant, and cost competitive for a variety of structural applications.

Several existing models for predicting the behavior of short-fiberreinforced composites were evaluated to determine the applicability to hybrid foams. None of these models accurately fit the experimental data, indicating that the behavior of hybrid composite foams involves mechanisms more complex than these models can represent. This deviation suggests that a better understanding is required to model the mechanisms of fiber reinforcement in foams, and the dependence on fiber type, fiber orientation, and critical length. Thus, considerable room for further optimization remains. An empirical approach may produce incremental improvements, although a predictive

Please cite the article as: A. Desai, M.L. Auad, H. Shen, and S.R. Nutt, “**Mechanical Behavior of Hybrid Composite Phenolic Foam,**” *J. Cellular Plastics* 44 [1] (2008) 15-36. DOI: **10.1177/0021955X07078021**



model for mechanical properties of composite foams is sorely lacking. A mechanistic model incorporating basic material parameters, such as fiber strength/ stiffness, fiber length, fiber loading, orientations, and foam density would be desirable, although the stochastic nature of the microstructure might be prohibitively complex. The authors are currently pursuing the SLAW approach to simulate and predict the complex behavior of hybrid foams.

Acknowledgements: The authors are grateful to the Merwyn C. Gill Foundation for financial support.

References:

1. Martin, Y.M.C., Wang, X., Schultheisz, C.R. and He, J. (2005). Prediction and Three-dimensional Monte-Carlo Simulation for Tensile Properties of Unidirectional Hybrid Composites, *Comp. Sci. Tech.*, 65(11–12): 1719–1727.
2. Prem, E.J.B., Savithri, S., Pillai, U.T.S. and Pai, B.C. (2005). Micromechanical Modeling of Hybrid Composites, *Polymer*, 46(18): 7478–7484.
3. Shan, Y. and Liao, K. (2002). Environmental Fatigue Behavior and Life Prediction of Unidirectional Glass–carbon/epoxy Hybrid Composites, *Int. J. Fatigue*, 24(8): 847–859.
4. Idicula, M., Neelakantan, N.R., Oommen, Z., Joseph, K. and Thomas, S. (2005). A Study of the Mechanical Properties of Randomly Oriented Short Banana and Sisal Hybrid Fiber Reinforced Polyester Composites, *J. App. Poly. Science*, 96(5): 1699–1709.
5. Shao-Yun, F., Yiu-Wing, M., Lauke, B. and Chee-Yoon, Y. (2002). Synergistic Effect on the Fracture Toughness of Hybrid Short Glass Fiber and Short Carbon Fiber Reinforced Polypropylene Composites, *Mater. Sci. Eng. (A)*, 323(1–2): 326–335.
6. Mao, J., Chang, J., Chen, Y. and Fang, D. (1998). Review of Phenolic Foam, *Chem. Ind. Eng.*, 15(3): 38–43.
7. Shen, H., Lavoie, A.J. and Nutt, S.R. (2003). Enhanced Peel Resistance of Fiber Reinforced Phenolic Foams, *Comp. A: Appl. Sci. Manufact.*, 34(10): 941–948.
8. Knop, A. and Scheip, W. (1979). *Chemistry and Application of Phenolic Resins*, Springer, New York.
9. Takanori, K. (1993). JP 05-286069.
10. Manabu, H. (1993). JP 05-318506.
11. Halpin, J.C. and Kardos, J.L. (1972). Moduli of Crystalline Polymers Employing Composite Theory, *J. Appl. Phys.*, 43(5): 2235–2241.
12. Cohen, M.I. (1994). WO 94/04604.
13. Nutt, S.R. and Shen, H. (2005). US Patent 6,841,584.
14. Boeing Part Specification (BPS) D124. (1991). Air, Panels and Plenum Insulation, Rigid Plastic Foam, for Low Pressure Systems, Boeing.
15. Gibson, L.J. and Ashby, M.F. (1997). *Cellular Solids: Structure and Properties*, Cambridge, UK.

Please cite the article as: A. Desai, M.L. Auad, H. Shen, and S.R. Nutt, “**Mechanical Behavior of Hybrid Composite Phenolic Foam,**” *J. Cellular Plastics* 44 [1] (2008) 15-36. DOI: **10.1177/0021955X07078021**



16. Technical Guide of Nomex Brand Fiber (2002). Technical information, DuPont.
17. Lauscha Fiber International (2002). Technical data sheet.
18. Shen, H., Nutt, S.R. and Hull, D. (2004). Direct Observation and Measurement of Fiber Architecture in Short Fiber-polymer Composite Foam through Micro-CT Imaging, *Comp. Sci. Tech.*, 64(13–14): 2113–2120.
19. Zenkert, D. (1995). *An Introduction to Sandwich Construction*, Chamelon, London.
20. Shen, H. and Nutt, S.R. (2003). Mechanical Characterization of Short Fiber Reinforced Phenolic Foam, *Comp. Part A*, 34(9): 899–906.
21. Kaynak, C., Arikian, A. and Tincer, T. (2003). Flexibility Improvement of Short Glass Fiber Reinforced Epoxy by using a Liquid Elastomer, *Polymer*, 44(8): 2433–2439.
22. Vaikhanski, L. and Nutt, S.R. (2003). Fiber-reinforced Composite Foam from Expandable PVC Microspheres, *Comp. Part A*, 34(12): 1245–1253.
23. Broek, D. (1982). *Elementary Engineering Fracture Mechanics*, Dordrecht, Martinus Nijhoff, 469.
24. FR-6700® Series Foam Product (2004). General Plastics Manufacturing Company.
25. Robinson, I.M. and Robinson, J.M. (1994). The Influence of Fiber Aspect Ratio on the Deformation of Discontinuous Fiber-reinforced Composites, *J. Mater. Sci.*, 29(18): 4663–4677.
26. Sarasua, J.R., Remiro, P.M. and Pouyet, J. (1995). The Mechanical Behavior of PEEK Short Fiber Composites, *J. Mater. Sci.*, 30(13): 3501–3508.
27. Radesh Kumar, C., George, K.E. and Thomas, S. (1996). Morphology and Mechanical Properties of Thermoplastic Elastomers from Nylon-nitrile Rubber Blends, *J. Appl. Poly. Sci.*, 61(13): 2383–2396.
28. Halpin, J.C. and Tsai, S.W. (1967). Effects of Environmental Factors on Composite Materials, Rep. No: AFML-TR-67-423, Air Force Materials Laboratory, Wright Patterson Air Force Base, Ohio.
29. Rosen, B.W. (1965). *Fiber Composite Materials*, American Society for Metals, Metals Park, OH, p. 58.
30. Hirsch, T.J. (1962). *J. Am. Con. Inst.*, 59: 427–451.
31. Kalaprasad, G., Joseph, K. and Thomas, S. (1997). Theoretical Modelling of Tensile Properties of Short Sisal Fiber-reinforced Low-density Polyethylene Composites, *J. Mat. Sci.*, 32(16): 4261–4267.
32. Hyer, M.W. and White, S.R. (1998). *Stress Analysis of Fiber-reinforced Composite Materials*, McGraw-Hill, New York.
33. Mendez, P. and Ordonez, F. (2005), Scaling Laws from Statistical Data and Dimensional Analysis, *J. Appl. Mech.*, 72: 648–657.